CHIN. PHYS. LETT. Vol. 36, No. 4 (2019) 043201

Experimental Investigation of the Electromagnetically Induced-Absorption-Like Effect for an N-Type Energy Level in a Rubidium BEC *

Khan Sadiq Nawaz[1,2], Cheng-Dong Mi(米成栋)[1,2], Liang-Chao Chen(陈良超)[1,2], Peng-Jun Wang(王鹏军)[1,2], Jing Zhang(张靖)[1,2]**

[1]*State Key Laboratory of Quantum Optics and Quantum Optics Devices, Institute of Opto-Electronics, Shanxi University, Taiyuan 030006*

[2]*Collaborative Innovation Center of Extreme Optics, Shanxi University, Taiyuan 030006*

(Received 23 December 2018)

We study the electromagnetically induced-absorption-like (EIA-like) effect for an n-type system in an ^{87}Rb Bose–Einstein condensate (BEC) using the absorption imaging technique for coupling and driving lasers operating at the D_1 and D_2 lines of ^{87}Rb. The coherent effect is probed by measuring the number of atoms remaining after the BEC is exposed to strong driving fields and a weak probe field. The absorption imaging technique accurately reveals the EIA-like effect of the n-type system. This coherent effect in an n-type system is useful for optical storage, tunable optical switching, and so on.

PACS: 32.70.Jz, 32.10.Fn, 32.60.+i DOI: 10.1088/0256-307X/36/4/043201

Modifying the absorptive or dispersive properties of a medium using coherent driving fields to study coherent phenomena is a hot topic in atomic and optical physics. These phenomena are not only of fundamental interest for understanding light-matter interaction but also applicable in various light-matter-interaction-based devices. The schemes devised for observation of such effects include n-type, ladder-type, Λ-type, V-type, cascade and tripod. In such systems, electromagnetically induced transparency (EIT),[1,2] coherent population trapping,[3] superluminal,[4] and subluminal[5] light propagation, electromagnetically induced absorption (EIA) due to spontaneously generated coherence,[6–9] storage of light,[10,11] coherent nonlinear optics at low light levels[12–14] and lasing without inversion (LWI)[15] have been studied deeply. For this purpose, hot as well as cold atoms are used. However, a BEC is a useful tool for observing various phenomena that are not possible in hot atoms due to the Doppler shift. BECs also allow the absorption imaging technique in addition to transmission or scattering techniques for the probing of such coherent phenomena inside the medium. Such an absorption imaging technique is not suitable for hot atoms as they are moving at high speeds. The absorption imaging studies of the EIT[16] and EIA[17] in a BEC of ^{87}Rb have already proved that this technique is capable of precisely revealing the coherent properties of the systems under study in ultracold atoms.

In this work, we study the EIA-like effect for an n-type system in a ^{87}Rb BEC as shown in Fig. 1. A similar n-type system studied here is already discussed,[18–20] where the probe light transmission as a function of frequency detuning is measured. Our system, however, is different from the previous systems[18,19] because in our system the driving and coupling lasers share the same lower ground level in the n-type system while in the system of Ref. [18,19] the driving and probe lasers share the same lower level. Also, we measure the number of remaining atoms in the absorption image after the BEC is exposed to strong driving and coupling lasers and weak probe lasers, while they measure the transmission spectrum of the probe laser directly using a photodetector. In principle, this absorption imaging technique is equivalent to the measurement of the transmission of the weak probe beam. In transmission spectroscopy, absorption of the probe reduces the laser transmission while in absorption imaging, the number of atoms reduces in the BEC due to heating caused by the probe laser.

As shown in Fig. 1(b), the coupling laser at frequency ω_c, locked between the lower ground state $F = 1$ and the $F' = 1$ state of the D_1 line and the weak probe laser at frequency ω_p, is optically phase-loop locked to the coupling laser and its frequency may be scanned from the $F = 2$ to $F' = 1$ transition, together forming a Λ-type system. We construct the n-type system by adding a driving laser to couple the transition between the $|F = 1\rangle$ to $|F' = 2\rangle$ transition of the D_2 line. Since the BEC is prepared in the $|F = 2, m_F = 2\rangle$ state, we lock the driving laser to the $|F = 1\rangle$ to $|F' = 2\rangle$ transition of the D_2 line represented by ω_d, as opposed to the study in Ref. [18-20] The Λ-type system results in the standard EIT (Fig. 2(a)) but adding the driving laser transforms the EIT into an EIA-like shape (Fig. 2(c)), and it is quite different from the EIA. This n-type configuration resembles the absorption line-shape of EIA just as Autler–Townes splitting in a three-level system resembles the line-shape of EIT although having different origins.[18,21]

*Supported by the National Key Research and Development Program of China under Grant No 2016YFA0301602, the National Natural Science Foundation of China under Grant Nos 11474188 and 11704234, the Fund for Shanxi '1331 Project' Key Subjects Construction, and the Program of Youth Sanjin Scholar.

**Corresponding author. Email: jzhang74@sxu.edu.cn

The Hamiltonian and the density matrix equation of motion for our system after the dipole and rotating wave approximations are, respectively, given by[22]

$$H = \sum_{a=1}^{4}(\hbar\omega_a|a\rangle\langle a|) - \frac{\hbar}{2}(\Omega_p e^{-i(\omega_p t)}|3\rangle\langle 1| + \Omega_c e^{-i(\omega_c t)}|3\rangle\langle 2| + \Omega_d e^{-i(\omega_d t)}|4\rangle\langle 2| + \text{H.c.}), \quad (1)$$

$$\dot{\rho}_{ij} = -\frac{i}{\hbar}\sum_{k=1}^{4}(H_{ik}\rho_{ij} - \rho_{ik}H_{kj}) - \frac{1}{2}\sum_{k=1}^{4}(\Gamma_{ik}\rho_{ij} + \rho_{ik}\Gamma_{kj}), \quad (2)$$

where Ω_p, Ω_c and Ω_d are the probe, coupling and driving laser Rabi frequencies, respectively, and ω_p, ω_c and ω_d are the laser frequencies. Equation (2) can now be solved for the coherence ρ_{31} in the steady state in the weak probe field limit, and supposing the atoms to be initially in the $|1\rangle$ state.[20,23] This coherence ρ_{31} between the states $|1\rangle$ and $|3\rangle$ is responsible for the probe absorption by the atoms. The steady state solution for the coherence is

$$\rho_{31} = \frac{\Omega_p(\gamma'_{21}\gamma'_{41} - \Omega_d^2)}{\gamma'_{31}(\gamma'_{21}\gamma'_{41} - \Omega_d^2) - \gamma'_{41}\Omega_c^2}, \quad (3)$$

where $\gamma'_{21} = -i\gamma_{21} + (\Delta_p - \Delta_c)$, $\gamma'_{31} = \Delta_p - i\gamma_{31}$, $\gamma'_{41} = \Delta_p - \Delta_c + \Delta_d - i\gamma_{41}$, $\Delta_p = \omega_{13} - \omega_p$, $\Delta_c = \omega_{23} - \omega_c$, and $\Delta_d = \omega_{42} - \omega_d$. From Eq. (3), we can see three dips in the transmission spectrum of the probe. The reason for the existence of such dips has been discussed.[18,19]

Here the EIA-like effect can be easily explained by the dressed state picture.[24–26] The driving and coupling lasers create three dressed states in this n-type system, which are connected by the weak probe laser, given by

$$|\beta_0\rangle = \frac{(-\Omega_d|3\rangle + \Omega_c|4\rangle)}{\sqrt{\Omega_c^2 + \Omega_d^2}},$$
$$|\beta_1\rangle = \frac{1}{\sqrt{2}}\Big(|2\rangle + \frac{\Omega_c}{\sqrt{\Omega_c^2 + \Omega_d^2}}|3\rangle + \frac{\Omega_d}{\sqrt{\Omega_c^2 + \Omega_d^2}}|4\rangle\Big),$$
$$|\beta_2\rangle = \frac{1}{\sqrt{2}}\Big(-|2\rangle + \frac{\Omega_c}{\sqrt{\Omega_c^2 + \Omega_d^2}}|3\rangle + \frac{\Omega_d}{\sqrt{\Omega_c^2 + \Omega_d^2}}|4\rangle\Big). \quad (4)$$

These dressed states have an energy separation of $\sqrt{\Omega_c^2 + \Omega_d^2}$ when both the driving and coupling lasers are at resonance. The introduction of the driving laser changes the EIT effect (Fig. 2(a)) in the Λ-type system created by the coupling laser ω_c and the weak probe laser ω_p[24–26] into the EIA-like effect for an n-type system. The probe gets absorbed at the positions of these three dressed states (Fig. 2(c)). The positions of these states can be controlled by the detuning and the power of the coupling and driving lasers. We study this system for various powers and detuning of the coupling and driving fields.

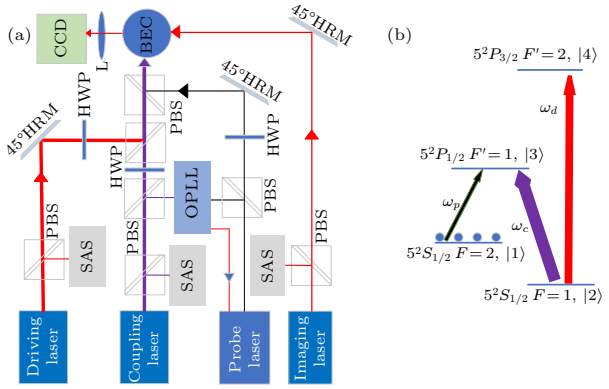

Fig. 1. Schematic diagram of experimental setup and energy levels. (a) The experimental setup. SAS: saturation absorption spectroscopy, PBS: polarizing beam splitter, OPLL: optical phase lock loop, HWP: half wave plate, L: focusing lens, 45°HRM: 45° highly reflecting mirror. (b) The n-type energy level, where the coupling and driving lasers are locked between the lower ground state and the $F' = 1$ state of the D_1 and the $F' = 2$ state of the D_2 line, while the probe is scanned across the $F = 2$ to $F' = 1$ transition.

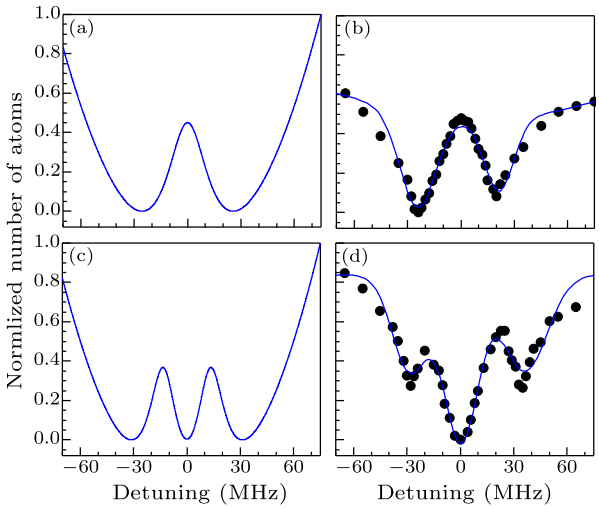

Fig. 2. The probe laser absorption profile for Λ-type and n-type systems. [(a), (b)] The theoretical and experimental results respectively for the Λ-type system. [(c), (d)] The theoretical and experimental results for the n-type system. The introduction of the driving laser changes the EIT effect into the EIA-like effect. The powers of the coupling and driving lasers in (b) and (d) are $P_c = 400\,\mu W$, $P_d = 200\,\mu W$ while the probe laser power is $P_p = 25\,\mu W$. The solid curves in the experimental plots are a guide for the eyes.

The experimental setup is shown in Fig. 1(a). We prepare the ^{87}Rb BEC having around 1×10^6 atoms in the ground $|F = 2, m_F = 2\rangle$ state after evaporative cooling in a crossed beam optical dipole trap operating at 1064 nm. In the Thomas–Fermi regime, the size of the BEC is approximately 20 µm. The coupling and driving laser beam waists ($\frac{1}{e^2}$ radius) are around 280 µm at the BEC position while the probe has a beam waist of 600 µm. Right after release from

the dipole trap, the BEC is exposed to the three laser fields simultaneously for a period of 0.01 ms. All of the three lasers interact with the n-type energy levels for the same amount of time in the ultracold atoms. The atoms are then imaged after 30 ms of free flight in the vacuum using an imaging beam and a CCD camera. The imaging laser is locked to the transition from the $F = 2$ state to the excited $F' = 3$ state of the D2 line and probes the number of atoms still remaining in the $F = 2$ state after being exposed to the three lasers. The number of remaining atoms is obtained from the absorption image. When the BEC is exposed to the three laser fields simultaneously, the strong absorption heats the atoms, which expand more quickly and escape the ultracold atomic cloud during the free flight before being imaged. Therefore, the spectrum of the number of remaining atoms as a function of the frequency detuning of the probe can be obtained, which corresponds to the transmission spectrum of the probe laser. Figures 2(b) and 2(d) are the experimental demonstration of how the addition of the driving laser converts the EIT into the EIA-like structure.

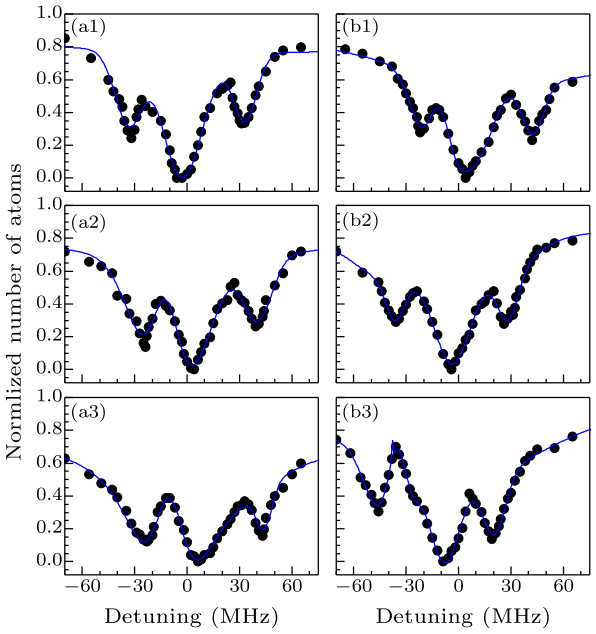

Fig. 3. The number of remaining atoms in the BEC as a function of the probe detuning for different detunings of the coupling and driving fields. The absorption images were taken 30 ms after exposing the BEC to the three laser fields. [(a1)–(a3)] The effect of driving laser detuning. [(b1)–(b3)] The effect of coupling laser detuning. (a1) $\Delta_c = 0$, $\Delta_d = +10$ MHz; (a2) $\Delta_c = 0$, $\Delta_d = -10$ MHz; (a3) $\Delta_c = 0$, $\Delta_d = -20$ MHz; (b1) $\Delta_c = +10$ MHz, $\Delta_d = 0$; (b2) $\Delta_c = -10$ MHz, $\Delta_d = 0$. (b3) $\Delta_c = -20$ MHz, $\Delta_d = 0$. The probe laser power is $P_p = 25\,\mu$W while the coupling and driving laser powers are $P_c = 400\,\mu$W and $P_d = 200\,\mu$W, respectively. High powers of coupling and driving lasers are used to achieve deep absorption dips on the two sides of the central dip. The detunings of both the driving and coupling lasers are changed using acousto-optic modulators (AOMs). The solid curves in the plots are a guide for the eyes.

Here we further study this system for various powers and detunings of the coupling and driving fields. Figure 3 shows the behavior of the three dips for various driving and coupling laser detunings. Figures 3(a1)–3(a3) list different detunings of the driving laser while the coupling laser is held at resonance. Similarly, Figures 3(b1)–3(b3) list the cases where we change the coupling laser detuning and the driving laser is held at resonance. We notice that the shift direction of these dips for the negative detuning of the coupling laser and the positive detuning of the driving laser is the same. Similarly, the effect of the positive detuning of the coupling laser is similar to that of the negative detuning of the driving laser showing the competition between the two lasers on the energy levels of the dressed states of Eq. (4). This agrees with the theoretical predictions made.[20] The coherence ρ_{31} of Eq. (3) also predicts such behavior of the probe absorption with respect to detuning of the driving or coupling laser. For a very large detuning of the driving laser, the effect of the driving laser will vanish and the system will act like a Λ-type system if there is no driving laser, and the single EIT feature reappears as in the previous report.[20] This kind of n-type configuration is capable of tunable optical switching of the probe laser by controlling the detuning of the coupling and driving lasers.

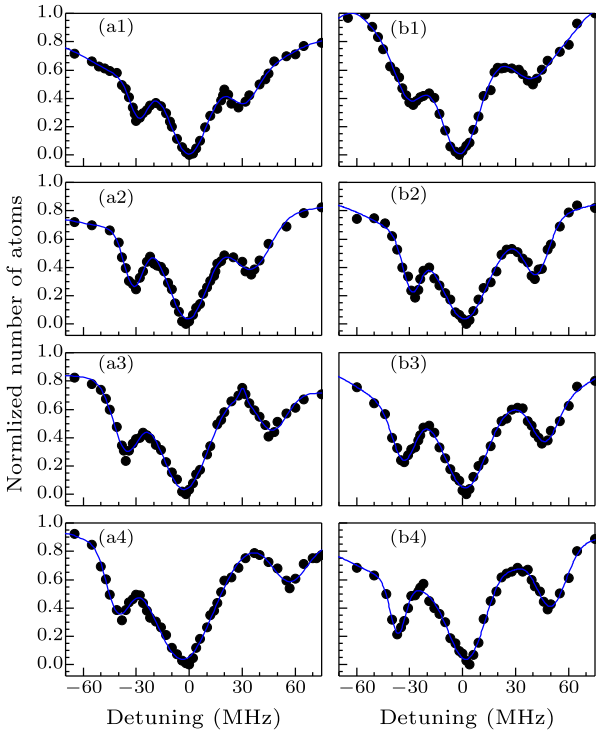

Fig. 4. The number of remaining atoms in the BEC as a function of probe detuning for the various powers of the coupling and driving fields. [(a1)–(a4)] The effect of changing the driving laser power with the coupling laser held at constant power. [(b1)–(b4)] The effect of changing coupling laser power with the driving laser held at constant power. (a1) $P_c = 400\,\mu$W, $P_d = 100\,\mu$W; (a2) $P_c = 400\,\mu$W, $P_d = 200\,\mu$W; (a3) $P_c = 400\,\mu$W, $P_d = 400\,\mu$W; (a4) $P_c = 400\,\mu$W, $P_d = 800\,\mu$W; (b1) $P_c = 100\,\mu$W, $P_d = 400\,\mu$W; (b2) $P_c = 200\,\mu$W, $P_d = 400\,\mu$W; (b3) $P_c = 600\,\mu$W, $P_d = 400\,\mu$W; (b4) $P_c = 800\,\mu$W, $P_d = 400\,\mu$W, $P_p = 25\,\mu$W, and $\Delta_c = 0$, $\Delta_d = 0$. The solid curves in the plots are a guide for the eyes.

Figure 4 shows the effects of coupling and driv-

ing laser powers on the three dips. Since the mixing strength of each uncoupled state in the three dressed states is scaled by the strength of the corresponding laser Rabi frequencies,[27] the change of power will shift the positions of these dressed states. When we change the power of the driving laser while holding the coupling laser power constant (Figs. 4(a1)–4(a4)), we can observe that the dip on the blue side of the center frequency shifts slightly more towards the blue side as compared to the dip on the red side of the central dip. Similar behavior can be observed when the coupling laser power is changed with the driving laser power held constant (Figs. 4(b1)–4(b4)). This asymmetry could be due to the hyperfine structure of the D-lines of ^{87}Rb atoms.[23] However, Eq. (4) predicts an equal shift of the two side-dips from the central dip because Eq. (4) does not take into account the effects of the other hyperfine levels. The three dips persist even for a weak driving laser power of approximately $P_{\rm d} = 10\,\mu$W while $P_{\rm c} = 400\,\mu$W, showing that such a small driving laser power can suppress the EIT by introducing the dressed states given in Eq. (4).

In conclusion, we have studied the EIA-like effect for an n-type system in the ^{87}Rb BEC using the absorption imaging technique. We are able to recover the characteristics of the coherently driven n-type system using this absorption imaging technique, and it is found that this technique of probing physical phenomena in BECs is equally powerful to transmission or scattering techniques provided that the BEC preparation process produces a stable BEC in each run. This n-type system configuration can be used for tunable optical switching. Moreover, a one-dimensional superradiance lattice of a BEC based on a configuration of standing wave-coupled EIT is realized experimentally.[28] Therefore, this EIA-like effect in an n-type system can also be used for studying directional scattering in a superradiance lattice.

References

[1] Harris S E 1997 *Phys. Today* **50** 36
[2] Cheng H, Zhang S S, Xin P P, Cheng Y and Liu H P 2016 *Chin. Phys. B* **25** 114203
[3] Arimondo E 1996 *Progress in Optics* (Amsterdam: Elsevier Science) p 257
[4] Akulshin A M, Barreiro S and Lezama A 1999 *Phys. Rev. Lett.* **83** 4277
[5] Budker D, Kimball D F, Rochester S M and Yashchuk V V 1999 *Phys. Rev. Lett.* **83** 1767
[6] Liu C P, Gong S Q, Fan X J and Xu Z Z 2004 *Opt. Commun.* **231** 289
[7] Xia H R, Ye C Y and Zhu S Y 1996 *Phys. Rev. Lett.* **77** 1032
[8] Taichenachev A V, Tumaikin A M and Yudin V I 1999 *Phys. Rev. A* **61** 011802
[9] Valente P, Failache H and Lezama A 2003 *Phys. Rev. A* **67** 013806
[10] Phillips D F, Fleischhauer A, Mair A, Walsworth R L and Lukin M D 2001 *Phys. Rev. Lett.* **86** 783
[11] Scully M O, Zhu S Y and Gavrielides A 1989 *Phys. Rev. Lett.* **62** 2813
[12] Babin S A, Podivilov E V, Shapiro D A, Hinze U, Tiemann E and Wellegehausen B 1999 *Phys. Rev. A* **59** 1355
[13] Braje D A, Balic V, Goda S, Yin G Y and Harris S E 2004 *Phys. Rev. Lett.* **93** 183601
[14] Harris S E, Field J E and Imamoglu A 1990 *Phys. Rev. Lett.* **64** 1107
[15] Kocharovskaya O 1992 *Phys. Rep.* **219** 175
[16] Chen L C, Yang G Y, Meng Z M, Huang L H and Wang P J 2017 *J. Quantum Opt.* **23** 246 (in Chinese)
[17] Yang G Y, Chen L C, Mi C D, Wang P J and Zhang J 2018 *J. Quantum Opt.* **24** 156 (in Chinese)
[18] Kong L B, Tu X H, Wang J, Zhu Y and Zhan M S 2007 *Opt. Commun.* **269** 362
[19] Kang H, Wen L and Zhu Y 2003 *Phys. Rev. A* **68** 063806
[20] Wan R G, Kou J, Jiang L, Kuang S Q, Jiang Y and Gao J Y 2011 *Opt. Commun.* **284** 1569
[21] Peng B, Özdemir Ş K, Chen W, Nori F and Yang L 2014 *Nat. Commun.* **5** 5082
[22] Scully M O and Zubairy M S 1997 *Quantum Optics* (Cambridge: Cambridge University Press)
[23] Sheng J, Yang X, Wu H and Xiao M 2011 *Phys. Rev. A* **84** 053820
[24] Mahmoudi M, Fleischhaker R, Sahrai M and Evers J 2008 *J. Phys. B: At. Mol. Opt. Phys.* **41** 025504
[25] Hamedi H R, Radmehr A and Sahrai M 2014 *Phys. Rev. A* **90** 053836
[26] Yang X, Ying K, Niu Y and Gong S 2015 *J. Opt.* **17** 045505
[27] Cohen-Tannoudji C, Dupont-Roc J and Grynberg G 2004 *Atom-Photon Interactions, Basic Processes and Applications* (Weinheim: Wiley)
[28] Chen L C, Wang P J, Meng Z M, Huang L H, Cai H, Wang D W, Zhu S Y and Zhang J 2018 *Phys. Rev. Lett.* **120** 193601